

Influence of Meteorological Factors on the Potential Evapotranspiration in Yanhe River Basin, China

Running title: ET_0 as affected by meteorological parameters

Yu Luo^{1,3}, Peng Gao^{1,2,3}, Xingmin Mu^{1,2,3}, Dexun Qiu^{1,3}

¹ State Key Laboratory of Soil Erosion and Dryland Agriculture on Loess Plateau, Institute of Soil and Water Conservation, Chinese Academy of Sciences and Ministry of Water Resources, 26 Xinong Road, Yangling, 712100, Shanxi Province, China.

² Institute of Soil and Water Conservation, Chinese Academy of Sciences and Ministry of Water Resources, Northwest A & F University, 26 Xinong Road, Yangling, 712100, Shanxi Province, China.

³ University of Chinese Academy of Sciences, Beijing, 100049, China

Corresponding Author:

address and email

Prof. Dr. Peng Gao

E-Mail: gaopeng@ms.iswc.ac.cn

Address: State Key Laboratory of Soil Erosion and Dryland Farming on the Loess Plateau, Northwest A&F University, 26 Xinong Road, Yangling, 712100, Shaanxi Province, China
Phone: +86-29-8701-2875

Prof. Dr. Xingmin Mu

E-Mail: xmmu@ms.iswc.ac.cn

Address: State Key Laboratory of Soil Erosion and Dryland Farming on the Loess Plateau, Northwest A&F University, 26 Xinong Road, Yangling, 712100, Shaanxi Province, China
Phone: +86-29-8701-2411

Abstract

Potential evapotranspiration (ET_0) is an essential component of the hydrological cycle, and quantitative estimation of the influence of meteorological factors on ET_0 can provide a scientific basis for studying the impact mechanisms of climate change. In the present research, the Penman-Monteith method was used to calculate ET_0 . The Mann-Kendall

statistical test with the inverse distance weighting were used to analyze the spatiotemporal characteristics of the sensitivity coefficients and contribution rates of meteorological factors to ET_0 to identify the mechanisms underlying changing ET_0 rates. The results showed that the average ET_0 for the Yanhe River Basin, China from 1978–2017 was 935.92 mm. Save for a single location (Ganquan), ET_0 increased over the study period. Generally, the sensitivity coefficients of air temperature (0.08), wind speed at 2 m (0.19), and solar radiation (0.42) were positive, while that of relative humidity was negative (-0.41), although significant spatiotemporal differences were observed. Increasing air temperature and solar radiation contributed 1.09% and 0.55% of the observed rising ET_0 rates, respectively; whereas decreasing wind speed contributed -0.63%, and relative humidity accounted for -0.85%. Therefore, it was concluded that the decrease of relative humidity did not cause the observed ET_0 increase in the basin. The predominant factor driving increasing ET_0 was rising air temperatures, but this too varied significantly by location and time (intra- and interannually). Decreasing wind speed at Ganquan Station decreased ET_0 by -9.16%, and was the primary factor underlying the observed, local “evaporation paradox.” Generally, increases in ET_0 were driven by air temperature, wind speed and solar radiation, whereas decreases were derived from relative humidity.

Keywords: climate change, changing meteorological factors, potential evapotranspiration, sensitivity coefficient, contribution rate, dominant factor

1. INTRODUCTION

According to the fourth assessment report of the Intergovernmental Panel on Climate Change (IPCC, 2007), the Earth's surface air temperature increased at a rate of $0.13^{\circ}\text{C}\cdot\text{decade}^{-1}$ from 1956–2005. Warming temperatures intensify hydrological cycling and affect the spatiotemporal allocation of water resources, increasing the frequency and intensity of water-related disasters (Zhou, 2019) and posing challenges to people's safety, socioeconomic development, and environmental security. Therefore, hydrological research is of utmost importance.

Evapotranspiration (ET), composed of water evaporation and transpiration from the surface, water, and plants, is an essential component of the water cycle, with corresponding control over the balances of water and energy. In practical applications, the concepts are divided into *actual* and *potential* (ET_0), where the former refers to ET under the true conditions of the surface, and latter describes ET levels when the surface is theoretically supplied with limitless water (FAO, 1998). ET_0 represents the limit value of actual ET in a region (Li, 2013), determines the dry and wet condition of a basin, and is an important indicator for estimating basin ET capacity (Zhou, 2019). Although ET under warming climates has been increasing in some regions, such as western Africa (Onyutha, 2016), Israel (Cohen et al., 2002), and southern China (Yin et al., 2010), ET_0 is largely decreasing around the globe in a phenomenon known as the "evaporation paradox" (Roderick & Farquhar, 2002; Roderick & Farquhar, 2004; Burn & Hesch, 2007; Fu et al., 2009). Scholars exploring the causes of changes in ET_0 have found that the decline in ET_0 in Australia (Roderick & Farquhar, 2002), Iran (Dinpashoh et al., 2011), and southern Canada (Burn & Hesch, 2007) were mainly caused by wind speed; whereas a decline in ET_0 in India was most closely related to relative humidity (Chattopadhyay & Hulme, 1997). In China, the most critical factor linked to the decline of ET_0 is water vapor pressure (Liu et al., 2012); however, due to the large geographical differentiation of natural conditions across the diverse regions of China, the drivers of ET_0 display significant spatial heterogeneity. ET_0 of the Yellow River Basin has been increasing, with patterns most closely associated with air temperature, followed by incoming solar radiation (Liu et al., 2010). The most important meteorological factor for ET_0 in the Yangtze River Basin was relative humidity (Gong et al., 2006), but decreases in solar radiation and wind speed were the main factors influencing lowered levels of ET_0 (Wang et al., 2007). ET in the upper reaches of the Heihe River Basin was also most correlated to relative humidity, but the observed changes were mainly driven by wind speed (Luo et al.,

2016). The observed decrease of ET_0 on the Qinghai-Tibet Plateau was related to a decrease of wind speed as well, in addition to a decrease in net radiation, and increase in air temperature (Zhang et al., 2007). The increasing ET_0 of the Loess Plateau was caused by the combined effect of rising air temperatures and declining in relative humidity, wind speed, and sunshine hours (Li et al., 2012). As indicated by the varied response of ET_0 to the complexities of the changing climate across spatially heterogeneous areas, the precise influence of climate factors on ET_0 are still highly uncertain and deserving of further exploration. Further, Liu et al. (2009) found that the change of ET_0 was not only affected by the climate sensitivity coefficient but is also related to the changing trend of meteorological factors. Thus, only by combining the sensitivity coefficient and contribution rate can we systematically and quantitatively analyze the driving mechanisms of change for ET_0 (Su et al., 2015).

Since the 1990s, climate change and anthropogenic activity have had a pronounced impact on the hydrological cycle of the Loess Plateau. The Yanhe River Basin (YRB), a typical watershed in the hilly and gully region of the Loess Plateau, provides an optimal opportunity for a more in-depth understanding of the impacts of climate change on ET_0 in a region of great significance for understanding the allocation of water resources and components of the water cycle for the region. Therefore, the YRB was selected as the study area for the present research. The Penman-Monteith method was used to calculate ET_0 , with the objectives of analyzing sensitivity to four major meteorological variables and changing trends of various climate factors. Subsequently, the contribution of these factors were quantitatively estimated, so as to reveal the mechanisms of observed ET_0 changes in the YRB over the past 40 years. Broadly, this study contributes to a more thorough understanding of the impact mechanisms of climate change on the hydrological cycle, and provides a scientific basis for water resource evaluation and management, in addition to informing agricultural planting structures.

2. DATA AND METHODS

2.1 Study area

The YRB is a first-level tributary of the middle reaches of the Yellow River, extending 286.9 km over a total drainage area of 7725 km². It originates from Zhoushan, Tianciwan Township, Jingbian County, and proceeds to flow through four primary counties and cities—Zhidan, Ansai, Baota, and Yanchang—and enters the Yellow River near the bank of Nanhegou Township in Yanchang County. The YRB maintains a continental monsoon

climate, which is dry-windy in spring, warm-rainy in summer, cool-rainy in autumn, and cold-dry in the winter (Yang, 2019). Average annual levels are: precipitation, ~520 mm; air temperature, 8.8–10.2°C; evaporation 898–1678 mm; and sunshine duration, 2450 h (Jiao et al., 2017).

2.2 Data

The meteorological data in the present study were acquired from China Meteorological Data Network (<http://data.cma.cn/>), and included the daily average, maximum, and minimum air temperatures (T , T_{max} , and T_{min} , respectively), wind speed duration $\geq 10 \text{ m}\cdot\text{s}^{-1}$ (U_{10}), sunshine duration (n , in h), daily average relative humidity (RH), and the daily precipitation (P). The U_{10} was converted into wind speed of 2 m (U_2). Data were collected across a time series from 1978–2017, derived from the specific control hydrological station of Ganguyi, and meteorological stations in Jingbian, Wuqi, Zhidan, Ansai, Yan'an, Zichang, Yanchuan, Yanchang, Ganquan and Yichuan (Figure 1).

[Insert Figure 1]

2.3 ET_0

The Penman-Monteith method, a commonly accepted standard in the literature, was used in the present research to calculate ET_0 (Equation 1, Zhang et al., 2012):

$$ET_0 = \frac{0.408 \Delta (R_n - G) + \gamma \frac{900}{(T + 273)} U_2 (e_s - e_a)}{\Delta + \gamma (1 + 0.34 U_2)} \quad (1)$$

where ET_0 is potential evapotranspiration (mm); R_n is the net radiation ($\text{MJ}\cdot\text{mm}^{-2}\cdot\text{day}^{-1}$); G is the soil heat flux ($\text{MJ}\cdot\text{mm}^{-2}\cdot\text{day}^{-1}$); γ is the psychrometric constant ($\text{kPa}\cdot^\circ\text{C}^{-1}$); T is mean daily air temperature at 2-m height ($^\circ\text{C}$); U_2 is the wind speed duration of $2 \text{ m}\cdot\text{s}^{-1}$; e_s and e_a are saturation and actual vapor pressure (kPa), respectively; and Δ is the slope of the vapor pressure curve ($\text{kPa}\cdot^\circ\text{C}^{-1}$).

2.4 Calculation of sensitivity coefficient

The dimensionless sensitivity coefficient (S_i ; Mccuen, 1974; Beven, 1979; Rana & Katerji, 1998; Hupet & Vanclooster, 2001) was used to characterize the sensitivity of ET_0 to climate change. This method analyzes the impact of a single climatic factor on ET_0 , while holding all others constant, and is calculated according to Equation 2:

$$S_i = \frac{\partial ET_0}{\partial i} \frac{i}{ET_0} \quad (2)$$

where i is change in the climate factor being assessed, and $\partial ET_0 / \partial i$ is the partial derivative of ET_0 with respect to climate factor i .

A positive (negative) sensitivity coefficient indicates that ET_0 will increase (decrease) as the variable increases; and the absolute value of the sensitivity coefficient indicates the climatic factor's degree of influence. An S_i of -0.1, for example, indicates that a 10% increase (decrease) of factor i will cause a 5% decrease (increase) in ET_0 when the other meteorological variables are held constant. In the present study, the sensitivity coefficients of average air temperature, humidity, wind speed, and solar radiation were calculated and denoted as S_T , S_{RH} , S_{U_2} , S_{R_s} , respectively. In this study, we regarded March to May as spring, June to August as summer, September to November as autumn and December to February as winter. And the monthly and annual values of the sensitivity coefficients were obtained by averaging the daily sensitivity coefficients.

2.5 Calculation of contribution rate

In the research here, the contribution rate of climatic factors to ET_0 was indicated by multiplying S_i by the relative change rate of factor i (Yin et al., 2010), and computed according to Equations (3) and (4).

$$C_i = S_i \cdot R_i \quad (3)$$

$$R_i = \frac{N \cdot L_i}{M_i} 100\% \quad (4)$$

where C_i is the contribution rate of change of i to ET_0 (%), R_i is the relative rate of change of climatic factor i , N is the number of years in the study period, L_i is the linear trend rate of climatic factor i , and M_i is the average value of the climatic factor.

Similarly to S_i , positive (negative) C_i indicates the positive (negative) effect of climatic factor i on the change of ET_0 , and the greater its absolute value, the greater its contribution.

2.6 Analytical method

The non-parametric Mann-Kendall statistical test (Mann, 1945; Kendall, 1975) was used to detect the trends of the sensitivity coefficients, and resulting contribution rates of ET_0 in the YRB from 1978 to 2017. The inverse distance weighting method was used to further interpolate the sensitivity coefficient and contribution rate (Lin et al., 2002).

3. RESULTS

3.1 Temporal and spatial characteristics of ET_0 and meteorological factors

The changes in multi-year average monthly ET_0 and meteorological factors for the YRB are shown in Table 1. Averages from 1978–2017 were: air temperature, 9.59°C (maximum observed from June to August); RH, 60.05% (maximum observed from August to October); wind speed at 2 meters height, 1.16 m·s⁻¹ (maximum observed from March to May); solar radiation, 5645.81 MJ·mm⁻²·day⁻¹ (maximum observed from May to July); and precipitation, 495.19 mm (maximum observed from July to September). The results of the Mann-Kendall statistical test indicated that air temperature ($p < 0.01$), solar radiation, and precipitation showed an increasing trend with time, while RH and wind speed at 2 m height were decreasing. The average ET of YRB was 935.92 mm, peaking from May to July. Overall, ET_0 showed an increasing trend ($p < 0.1$), while ET_0 values for September–October were decreasing, although not at a statistically significant level.

[Insert Table 1]

Average annual air temperature of YRB from 1978 to 2017 presented a geographical distribution pattern of southeastern highs and northwestern lows, both of which increased over time (Figure 2). RH displayed highs in the west and east, and lows in the north and south. Only the Zichang and Yanchang stations showed an insignificant rising trend in RH, indicating that the YRB underwent significant warming and drying. U_2 reached lows in the east and west, highs to the north and south, with an overall downward trend save for the

Zichang, Yanchang, Yanchuan, and Yichuan stations showing an increase. The incoming solar radiation in the southeast was less than that in the south, and displayed a decreasing trend; whereas the solar radiation at Yan'an and Jingbian stations were the highest in the basin, showing an upward trend. Precipitation in the YRB had a distribution pattern of south > southeast > northwest, peaking at Yan'an and Ganquan stations. Save for the sole location of Yan'an, precipitation in the basin showed an upward trend. ET_0 was greatest in the south and least in the west. An upward trend was observed for all sites except Ganquan, where decreasing ET_0 levels with increasing air temperature indicated the local existence of the "evaporation paradox" phenomenon. It can be seen that the intra-annual characteristics of meteorological factors and ET_0 were variable, and spatial heterogeneity was significant throughout the study region.

[Insert Figure 2]

3.2 Sensitivity of ET_0 to meteorological factors

3.2.1 Temporal characteristics

S_T , S_{RH} , and S_{R_s} showed an intra-annual, single peak pattern, indicating that ET_0 was more sensitive to temperature conditions and sunshine duration in the summer over this scale. In addition, S_{U_2} showed a unimodal distribution, displaying that ET_0 was most sensitive to wind speed in the winter (Figure 3). On an interannual scale, S_T , S_{R_s} , and S_{U_2} increased, whereas S_{RH} decreased. The absolute value of S_{R_s} (0.42) was the largest of the factors examined, indicating that ET_0 was most sensitive to solar radiation, and increased by 4.2% for every 10% increase in solar radiation (while holding all other factors constant; Table 2). Examining each month across all years, S_T was positive except for in the winter, S_{RH} was consistently negative, S_{U_2} was positive throughout, and S_{R_s} was positive except for December. From analyses of the absolute values for the sensitivity coefficients of ET_0 , it was revealed that spring-summer values were mainly affected by solar radiation, and autumn-winter values by RH . Examining the M-K statistics, the monthly sensitivity coefficients of ET_0 in the YRB were variable: S_T increased over the study period, but declined in the months from March–September (save for April); S_{RH} decreased annually, but increased within each year from March–June; S_{U_2} increased overall, but decreased in the month of October; and S_{R_s} mostly decreased annually, but increased each year in April and May. It was found that over the 40-

year study period, the sensitivity of ET_0 to air temperature and wind speed had increased, while sensitivity to solar radiation and RH decreased. The sensitivity of ET_0 to the climatic factors examined varied by month throughout the year, and within each month of the year as well.

[Insert Figure 3]

[Insert Table 2]

3.2.2 Spatial characteristics

S_T , S_{U_2} , and S_{R_s} at each site in the YRB were positive values, whereas S_{RH} was the sole factor with a negative value. The absolute values of S_{RH} at the Jingbian, Zichang, Ansai, Yan'an, Ganquan, and Yichuan stations were the largest of all factors, indicating the importance of RH when determining ET_0 . The absolute values of S_{R_s} at the Wuqi, Zhidan, Yanchuan, and Yanchang stations were larger than elsewhere, confirming the importance of solar radiation on ET_0 . S_T tended to increase across all stations, save for Yan'an, Yanchang, and Yichuan; whereas S_{RH} tended to decrease save for Jingbian, Wuqi, Yan'an, and Ganquan stations. Except for Wuqi station, sensitivity of S_{U_2} was increasing. S_{R_s} was increased only at Ansai, Ganquan, and Wuqi stations, while decreasing at all other sites (Table 3). Therefore, the ET_0 of the YRB was most sensitive to RH and solar radiation, but this influence appears to be weakening. Contrarily, the sensitivity of ET_0 to air temperature and wind speed was small, but sensitivity is increasing.

The geographic distribution of ET_0 sensitivity to climatic factors was derived by spatial interpolation of the sensitivity coefficients for each station (Figure 4): S_T gradually decreased from SE to NW of the basin, peaking in the Yanchang area; S_{RH} increased from the central to SE and SW of the basin, reaching its maximum in Zhidan and Yanchuan, respectively; S_{U_2} was roughly opposite of S_{RH} , with a minimum in the Zhidan area; The distribution pattern of S_{R_s} was similar to that of S_{RH} , reaching maximums in Zhidan, Ganquan, and Yanchang. Thus, the sensitivity of ET_0 to each climate factor analyzed varied significantly by geographic location.

[Insert Table 3]

269

270 [Insert Figure 4]

271

272 3.3 Contribution rate of meteorological factors

273 On an annual scale, when the T increased by 14.35%, ET_0 increased by 1.09%. Since S_{RH} was
274 negative, an increase in RH by 2.09% led to a decrease in ET_0 by 0.85%. If U_2 decreased by
275 3.24%, ET_0 decreased by 0.63%; and when solar radiation increased by 1.32%, ET_0 increased
276 by 0.55%. Overall, air temperature was the dominant meteorological factor contributing to
277 ET_0 of the YRB from 1978–2017. From an intra-annual perspective, the increase in air
278 temperature in January and February led to an increase in ET_0 . The increases of ET_0 in March,
279 July, and August were most strongly correlated with the decrease in RH . The observed
280 increase in ET_0 in April and May was primarily caused by the decrease in U_2 . The most
281 significant driver of ET_0 in June was solar radiation, and the observed increase in ET_0 caused
282 by U_2 nearly offset the decrease driven by lowered RH . In September and October, the most
283 significant factor determining lowered ET_0 was the decline in solar radiation. T was the
284 dominant controlling factor of ET_0 in November. In November, although ET_0 had the greatest
285 level of sensitivity to RH , its contribution rate was only 0.03%, permitting the inference that
286 the decreasing trend of RH was not the primary cause of the observed decrease in ET_0 . The
287 most significant contribution to ET_0 in December was U_2 . In December, although ET_0 was
288 sensitive to RH , its decline did not lead to a decrease of ET_0 (Table 4).

289 Across the entire study region, a relatively equal change of a single climatic factor had
290 significantly variable contributions to ET_0 . For example, an increase of RH by 0.74%, lead to
291 a decrease in ET_0 at the Zichang station by 0.34%, and a decrease at the Yanchang station of
292 0.24% (Table 5). Through comparison, it was found that the dominant meteorological factor
293 at Jingbian, Zichang, Ansai, Ganquan, Yanchang, and Yanchuan stations was U_2 . Solar
294 radiation contributed the most to ET_0 at Wuqi station, and RH was the controlling factor at
295 Zhidan, Yan'an, and Yichuan stations. Air temperature contributed positively to the increase
296 of ET_0 across the entire basin, whereas the effects of RH , U_2 , and solar radiation on ET_0
297 displayed significant spatial variability. For example, the contribution rate of RH to the
298 recorded ET_0 values of Zichang and Yanchang stations was negative, but all other stations
299 recorded positive rates (Table 5). Because ET_0 of Zichang and Yanchang stations had a
300 negative sensitivity coefficient to RH , the observed increase in RH had a negative effect on
301 ET_0 . Conversely, other sites had a positive effect on ET_0 due to the decreasing levels of RH .

Thus, the geographic zonality each meteorological factor's contribution to ET_0 was significant. The influence of T and solar radiation on ET_0 gradually decreased from NW to SE of the basin, whereas U_2 displayed precisely the opposite pattern. The contribution of RH to ET_0 decreased radially from Zhidan to the surrounding areas (Figure 5). By combining Figures 2 and 5, it can be ascertained that the high ET in the Yan'an area was primarily driven by RH and solar radiation, whereas the low ET observed in the Zhidan area was mainly affected by U_2 . Because the sensitivity coefficient of ET_0 to RH in Ganquan was negative, the recorded decrease in RH had a positive effect on ET_0 . Similarly, the sensitivity coefficient of ET_0 to U_2 and solar radiation was positive, so the recorded decrease in U_2 and solar radiation contributed to the observed decrease in ET_0 . Therefore, the main factors behind the "evaporation paradox" phenomenon observed in Ganquan were decreasing values of U_2 and solar radiation.

[Insert Table 4]

[Insert Table 5]

[Insert Figure 5]

4. DISCUSSION

Previous studies have found that a combination of the changing meteorological factors, sensitivity coefficients, and contribution rates can more accurately analyze the drivers of ET_0 (Liu et al., 2009; Su et al., 2015).

4.1 Dominant factors of ET_0 variation in the YRB

The calculated absolute values (i.e., strengths) for the sensitivity coefficients of the climatic factors analyzed on ET_0 were solar radiation $> RH > U_2 > T$; however, sensitivities varied significantly by month. For example, the sensitivity coefficient of ET_0 to solar radiation in December was -0.01, but reached 0.7 in July and August from 1978 to 2017. Additionally, the sensitivity coefficient of T in the winter (December, January, February) was negative, but positive throughout the remainder of the year. Combined with the results of trend analysis of

meteorological factors, it was found that T still maintained a positive correlation with ET_0 , since T in the winter months was low as well.

The absolute values of the contribution rates for each meteorological factor to ET_0 were $T > RH > U_2 >$ solar radiation; and furthermore, these rates for each individual factor varied significantly by month. For example, the contribution rates of T to ET_0 for January, February, and December were 1.95%, 6.68%, and 1.46%, respectively; but these rates in June, July, and August were 0.64%, 1.16%, and 0.96%, thus indicating that the contribution of T to the increase of ET_0 was higher in winter months than in summer. Furthermore, although the sensitivity coefficient of ET_0 to T was small, its contribution was large as the significantly increasing trends of air temperature ($p < 0.01$) led to an increase of ET_0 . These findings are similar to the results of a study on ET_0 climate sensitivity coefficients in the Yellow River Basin (Liu et al., 2010). In the YRB, although the sensitivity coefficient of ET_0 to solar radiation was the greatest, its overall contribution to ET_0 was low due to its relatively stable rate over time.

Combined with precomplaint sensitivity analysis and contribution rate analysis in the present study, it can be seen that only by combining the sensitivity coefficients of changing meteorological factors to ET_0 , can we ascertain their true contribution rates for a more comprehensive understanding of the causes of changes in ET_0 .

In the present study, the multi-year average air temperature of the YRB showed an increasing trend, with a positive sensitivity coefficient, and a contribution rate of 1.09%. RH has displayed a decreasing trend with time, a sensitivity coefficient of -0.41, and contribution rate of -0.85%. It can be seen, however, that the decreasing trend of RH did not cause the increase in ET_0 in the YRB. U_2 also displayed a decreasing trend with time, a positive sensitivity coefficient of ET_0 , and a contribution rate of -0.63%. Solar radiation showed an increasing trend with time, a positive sensitivity coefficient, and contribution rate of 0.55%. Thus, it can be concluded that the negative contribution rates of meteorological factors ET_0 were less than the positive. Accordingly, ET_0 in the YRB has shown an increasing trend from 1978–2017 mostly related to T , U_2 , and solar radiation, whereas observed decreases in ET_0 were primarily driven by RH .

4.2 Evaporation paradox in the YRB

Another pertinent point was that although the ET_0 of the YRB showed an overall increasing trend, ET_0 at the Ganquan Station decreased, indicating a sole, local existence of the “evaporation paradox.” The absolute value of the sensitivity coefficients for the meteorological factors in the Ganquan area were $RH > \text{solar radiation} > U_2 > T$; and the absolute values of their contribution rates were $U_2 > RH > \text{solar radiation} > T$. In the Ganquan area, the increasing trend of air temperature was significant, but its corresponding contribution rate was relatively low. Solar radiation decreased with time, and its corresponding contribution rate to ET_0 was -0.74%, nearly offsetting the positive contribution rate of air temperature. The sensitivity coefficient for RH was -0.46, with a contribution rate of 1.37%, indicating that the downward trend of RH had a positive effect on ET_0 . Lastly, the sensitivity coefficient for U_2 was only 0.17, but its significant downward trend resulted in a contribution rate of -9.16%, making it the dominant factor driving the observed decreasing trend in ET_0 . This is similar to results found by Roderick & Farquhar (2002), Dinpashoh et al. (2011), Burn & Hesch (2007), and Luo et al. (2016).

5. CONCLUSIONS

In this paper, the effects of air temperature (T), relative humidity (RH), wind speed at 2 m (U_2), and solar radiation on the potential evapotranspiration (ET_0) in the Yanhe River Basin (YRB), China were quantitatively estimated using sensitivity coefficients and contribution rates, combined with the changing trend of meteorological factors observed from 1978–2017. The main conclusions of this study can be summarized as follows:

The absolute value of the sensitivity coefficients of ET_0 to meteorological factors in the YRB was $\text{solar radiation} > RH > U_2 > T$, although sensitivities displayed significant temporal (intra- and interannual) and spatial differences. The absolute values of the contribution rates for each meteorological factor were $T > RH > U_2 > \text{solar radiation}$. Similarly, the contribution rates for the same climatic factors displayed significant spatiotemporal heterogeneity.

The observed increase of ET_0 in the YRB was related to T , U_2 , and solar radiation; whereas decreases in ET_0 were mostly related to RH . The most dominant factor controlling ET_0 across the entire YRB was T , but this displayed significant spatiotemporal differences at local scales. The “evaporation paradox” phenomenon observed in the Ganquan area was driven primarily by wind speed.

It can be seen from this study only by combining the sensitivity coefficients of changing meteorological factors to ET_0 , with their respective contribution rates, can we systematically and quantitatively analyze the driving mechanisms of observed changes in ET_0 .

ACKNOWLEDGEMENTS

This work was founded by the National Key Research and Development Program of China, Grant/Award Number: 2016YFC0501707; Special Funds for Scientific Research Programs of the State Key Laboratory of Soil Erosion and Dryland Farming on the Loess Plateau, Grant/Award Number: A314021403-Q2.

DATA AVAILABILITY

The data that support the findings of this study are available from the corresponding author upon reasonable request.

REFERENCES

- Burn, D.H., Hesch, N.M., 2007. Trends in evaporation for the Canadian Prairies. *Journal of Hydrology*, 336(1-2):61-73.
- Beven, K., 1979. A sensitivity analysis of the Penman-Monteith actual evapotranspiration estimates. *Journal of Hydrology*, 44(3-4):169-190.
- Cohen, S., Ianetz, A., Stanhill, G., 2002. Evaporative climate changes at Bet Dagan, Israel, 1964-1998. *Agricultural and Forest Meteorology*, 111(2):83-91.
- Chattopadhyay, N., Hulme, M., 1997. Evaporation and potential evapotranspiration in India under conditions of recent and future climate change. *Agricultural and Forest Meteorology*, 87(1):55-73.
- Dinpashoh, Y., Hjahharia, D., Fakheri-Fard, A., Singh, V.P., Kahya, E., 2011. Trends in reference crop evapotranspiration over Iran. *Journal of Hydrology*, 399(3-4):422-433.
- Fu, G., Charles, S.P., Yu, J., 2009. A critical overview of pan evaporation trends over the last 50 years. *Climatic Change*, 97(1):193-214.
- Food and Agriculture Organization of the United Nations, 1998. *Crop Evapotranspiration: Guidelines for Computing Crop Requirements*. Italy: Food & Agriculture Org.
- Gong, L.B., Xu, C.Y., Chen, D.L., Halldin, S., Chen, Y.Q., 2006. Sensitivity of the Penman-Monteith reference evapotranspiration to key climatic variables in the Changjiang (Yangtze River) basin. *Journal of hydrology-amsterdam*, 329(3).
- Hupet, F., Vanclooster, M., 2001. Effect of the sampling frequency of meteorological variables on the estimation of the reference evapotranspiration. *Journal of Hydrology*, 243(3-4).
- IPCC, 2007. *Summary for Policymakers of Climate Change 2007: The Physical Science Basis*. Contribution of Working Group 1 to the Fourth Assessment Report of the Intergovernmental Panel on Climate Change. Cambridge: Cambridge University Press.
- Jiao, J.Y., Wang, Z.J., Wei, Y.H., Su, Y., Cao, B.T., Li, Y.J., 2017. Characteristics of erosion sediment yield with extreme rainstorms in Yanhe Watershed based on field. *Transactions of the Chinese Society of Agricultural Engineering*, 33(13): 159-167.
- Kendall, M.G., 1975. *Rank Correlation Measures*. Charles Grifn, London, UK. 202.

- Li X.C., 2013. Spatio-temporal variation of actual evapotranspiration in the pearl, Haihe and Tarim Basins of China. Nanjing, Jiangsu: Nanjing University of Information Science and Technology.
- Liu, C.M., Zhang, D., Liu, X.M., Zhao, C.S., 2012. Spatial and temporal change in the potential evapotranspiration sensitivity to meteorological factors in China (1960–2007). *Journal of Geographical Sciences*, 22(1).
- Liu, Q., Yang, Z.F., Cui, B.S., Sun, T., 2010. The temporal trends of reference evapotranspiration and its sensitivity to key meteorological variables in the Yellow River Basin, China. *Hydrological Processes*, 24(15):2171-2181.
- Luo, K.S., Tao, F.L., Deng, X.Z., Moiwu, J.P., 2016. Changes in potential evapotranspiration and surface runoff in 1981-2010 and the driving factors in Upper Heihe River Basin in Northwest China. *Hydrological Processes*, 31(1).
- Li, Z., Zheng, F.L., Liu, W.Z., 2012. Spatiotemporal characteristics of reference evapotranspiration during 1961–2009 and its projected changes during 2011–2099 on the Loess Plateau of China. *Agricultural & Forest Meteorology*, 154(none):147-155.
- Lin, Z.H., Mo, X.G., Li, H.X., Li, H.B., 2002. Comparison of Three Spatial Interpolation Methods for Climate Variables in China. *Acta Geographica Sinica*, 57(1):47-56.
- Liu, X.M., Zheng, H.X., Liu, C.M., Cao, Y.J., 2009. Sensitivity of the potential evapotranspiration to key climatic variables in the Haihe River Basin. *Resources Science*, 31(9):1470-1476
- Mccuen, R.H., 1974. A sensitivity and error analysis of procedures used for estimating evaporation1. *JAWRA Journal of the American Water Resources Association*, 10(3).
- Mann, H.B., 1945. Non-Parametric Test Against Trend. *Econometrica*. 13: 245-259.975
- Onyutha, C., 2016. Statistical analyses of potential evapotranspiration changes over the period 1930–2012 in the Nile River riparian countries. *Agricultural & Forest Meteorology*, 226-227:80-95.
- Roderick, M.L., Farquhar, G.D., 2002. The Cause of Decreased Pan Evaporation over the Past 50 Years. *Science*, 298(5597):1410-1411.
- Roderick, M.L., Farquhar, G.D., 2004. Changes in Australian pan evaporation from 1970 to 2002. *International Journal of Climatology*, 24(9):1077-1090.
- Rana, G., Katerji, N., 1998. A Measurement Based Sensitivity Analysis of the Penman-Monteith Actual Evapotranspiration Model for Crops of Different Height and in Contrasting Water Status. *Theoretical & Applied Climatology*, 60(1-4):141-149.
- Su, X.L., Song, Y., Niu, J.P., Ji, F., 2015. Sensitivity and attribution of potential evapotranspiration in Jinghuiqu irrigation district. *Journal of Natural Resources*, (1):115-123.
- Wang, Y., Jiang, T., Bothe, O., Fraedrich, k., 2007. Changes of pan evaporation and reference evapotranspiration in the Yangtze River basin. *Theoretical & Applied Climatology*, 90(1-2):13-23.
- Yin, Y.H., Wu, S.H., Chen, G., Dai, E.F., 2010. Attribution analyses of potential evapotranspiration changes in China since the 1960s. *Theoretical & Applied Climatology*, 101(1):19-28.
- Yang, X.N., 2019. Effects of landscape pattern on runoff and sediment in the Loess Plateau: A multi-scale study. Shanxi, Yangling: Dissertation Submitted to Northwest A & F University.
- Zhou J., 2019. Spatial and temporal variation of droughts over China based on various potential evapotranspiration formulas. Nanjing, Jiangsu: Nanjing University of Information Science and Technology.
- Zhang, Y.Q., Liu, C.M., Tang, Y.H., Yang, Y.H., 2007. Trends in pan evaporation and reference and actual evapotranspiration across the Tibetan Plateau. *Journal of Geophysical Research Atmospheres*, 112(D12).
- Zhang, X.L., Xiong, L.H., Lin, L., Long, H.F., 2012. Application of five potential evapotranspiration equations in Hanjiang Basin. *Arid Land Geography*, 35(02): 229-237.

481 **TABLES**

482 Table 1 Temporal characteristics of ET_0 and meteorological factors in Yanhe River Basin.

483 Table 2 Temporal characteristics of sensitivity coefficient of ET_0 to meteorological factors.

484 Table 3 MK statistics of Sensitivity coefficient of ET_0 to meteorological factors of Yanhe

485 River Basin.

486 Table 4 Temporal characteristic of contribution rate of meteorological factors to ET_0 in

487 Yanhe River Basin.

488 Table 5 Contribution rate of meteorological factors to ET_0 of stations in Yanhe River Basin.

489

490

491

492

493

494

495

496

497

498

499

500

501

502

503

504

505

506

507

508

509

510

511

512

513

514

31

32

Table1 Temporal characteristics of ET_0 and meteorological factors in Yanhe River Basin.

518

527

Table 2 Temporal characteristics of sensitivity coefficient of ET_0 to meteorological factors.

Time	Mean				M-K statistics			
	S_T	S_{RH}	S_{U2}	S_{Rs}	S_T	S_{RH}	S_{U2}	S_{Rs}
Jan.	-0.12	-0.51	0.32	0.09	1.33	-2.31	1.35	-0.56
Feb.	-0.05	-0.43	0.25	0.27	2.10	-1.77	0.56	-0.58
Mar.	0.04	-0.36	0.20	0.40	-0.33	1.82	2.82	-2.21
Apr.	0.09	-0.28	0.20	0.48	0.19	0.89	0.16	1.12
May.	0.12	-0.25	0.16	0.56	-0.19	1.07	0.30	0.09
Jun.	0.14	-0.24	0.13	0.63	-0.89	1.24	0.93	-0.07
Jul.	0.19	-0.28	0.09	0.70	-1.98	-0.02	1.70	-1.07
Aug.	0.22	-0.33	0.07	0.70	-2.54	-1.37	2.63	-2.83
Sep.	0.20	-0.44	0.09	0.61	-1.33	-2.77	1.37	-2.38
Oct.	0.13	-0.54	0.16	0.43	0.61	-1.82	-0.42	-0.37
Nov.	0.02	-0.62	0.29	0.16	1.00	-0.91	1.12	-1.19
Dec.	-0.07	-0.61	0.37	-0.01	2.84	-0.93	1.40	-1.21
Year	0.08	-0.41	0.19	0.42	0.82	-1.51	2.80	-1.82

Table3 MK statistics of Sensitivity coefficient of ET_0 to meteorological factors of Yanhe River Basin.

Station	Mean				M-K statistics			
	S_T	S_{RH}	S_{U2}	S_{Rs}	S_T	S_{RH}	S_{U2}	S_{Rs}
Jingbian	0.03	-0.46	0.26	0.34	1.12	3.05	2.89	-0.40
Wuqi	0.07	-0.36	0.17	0.43	0.56	2.07	-0.07	1.54
Zichang	0.07	-0.43	0.21	0.40	0.51	-3.57	1.42	-1.30
zhidan	0.08	-0.34	0.16	0.45	2.77	-1.21	2.10	-0.77
Ansai	0.08	-0.45	0.20	0.41	1.26	-0.16	1.07	0.72
Yan'an	0.08	-0.44	0.21	0.41	-1.56	0.05	1.33	-1.30
Ganquan	0.09	-0.46	0.17	0.45	2.68	3.38	0.54	1.72
Yanchuan	0.08	-0.28	0.17	0.44	0.61	-2.68	4.24	-3.36
Yanchang	0.10	-0.39	0.18	0.45	-1.72	-2.96	3.36	-3.22
Yichuan	0.09	-0.45	0.20	0.42	-1.56	-2.49	3.61	-3.84

Table 4 Temporal characteristic of contribution rate of meteorological factors to ET_0 in Yanhe River Basin.

Time	$R_T/\%$	$C_T/\%$	$R_{RH}/\%$	$C_{RH}/\%$	$R_{U2}/\%$	$C_{U2}/\%$	$R_{RS}/\%$	$C_{RS}/\%$
Jan.	-16.15	1.95	3.10	-1.59	2.34	0.76	0.53	0.05
Feb.	-123.61	6.68	8.25	-3.57	0.71	0.18	1.79	0.49
Mar.	63.48	2.86	-23.68	8.61	-4.53	-0.92	11.87	4.79
Apr.	12.65	1.15	-4.60	1.26	-23.55	-4.70	5.30	2.54
May.	2.77	0.33	-3.47	0.88	-22.31	-3.66	4.09	2.31
Jun.	4.57	0.64	-6.65	1.58	-11.78	-1.57	2.65	1.68
Jul.	6.11	1.16	-5.64	1.59	3.95	0.34	2.25	1.58
Aug.	4.48	0.96	-6.40	2.09	6.20	0.43	-2.29	-1.60
Sep.	9.70	1.95	-0.57	0.25	8.53	0.73	-9.20	-5.58
Oct.	11.47	1.44	4.18	-2.25	-5.09	-0.81	-6.80	-2.89
Nov.	66.20	1.26	-0.04	0.03	-4.10	-1.17	-2.04	-0.33
Dec.	-21.83	1.46	-4.92	3.01	10.80	3.96	2.62	-0.04
Year	14.35	1.09	2.09	-0.85	-3.24	-0.63	1.32	0.55

575
576
577
578
579
580
581

582 **Table 5 Contribution rate of meteorological factors to ET_0 of stations in Yanhe River**
583 **Basin.**

Station	$R_T/\%$	$C_T/\%$	$R_{RH}/\%$	$C_{RH}/\%$	$R_{U2}/\%$	$C_{U2}/\%$	$R_{RS}/\%$	$C_{RS}/\%$
Jingbian	27.75	2.02	-9.00	3.91	-31.68	-6.76	2.79	1.12
Wuqi	12.34	0.94	-3.92	1.35	-17.78	-2.82	8.81	3.95
Zichang	16.19	1.25	0.74	-0.34	10.52	2.10	-0.21	-0.08
zhidan	19.71	1.86	-4.56	2.10	-8.13	-1.40	4.27	1.90
Ansai	11.10	0.89	-1.46	0.40	-18.65	-3.13	2.23	0.98
Yan'an	12.91	1.25	-7.57	2.93	0.16	0.03	4.43	1.98
Ganquan	18.00	0.54	-2.99	1.37	-35.71	-9.16	-2.18	-0.74
Yanchuan	8.27	0.54	-0.51	0.18	40.06	6.90	-1.17	-0.50
Yanchang	4.70	0.39	0.74	-0.24	34.65	6.51	-3.42	-1.48
Yichuan	15.34	1.33	-4.67	2.12	8.13	1.64	-2.58	-1.09

584

585 **FIGURE LEGENDS**

586 Figure 1 Location of the Yanhe River Basin and the meteorological stations used in this study
587 (black dots).

588 Figure 2 Spatial distribution of contribution rate of each meteorological factor.

589 Figure 3 Characteristics of average daily sensitivity coefficient of ET_0 to meteorological
590 factors.

591 Figure 4 Spatial distribution of sensitivity coefficients of ET_0 to meteorological factors.

592 Figure 5 Spatial distribution of contribution rate of each meteorological factor.

593

594

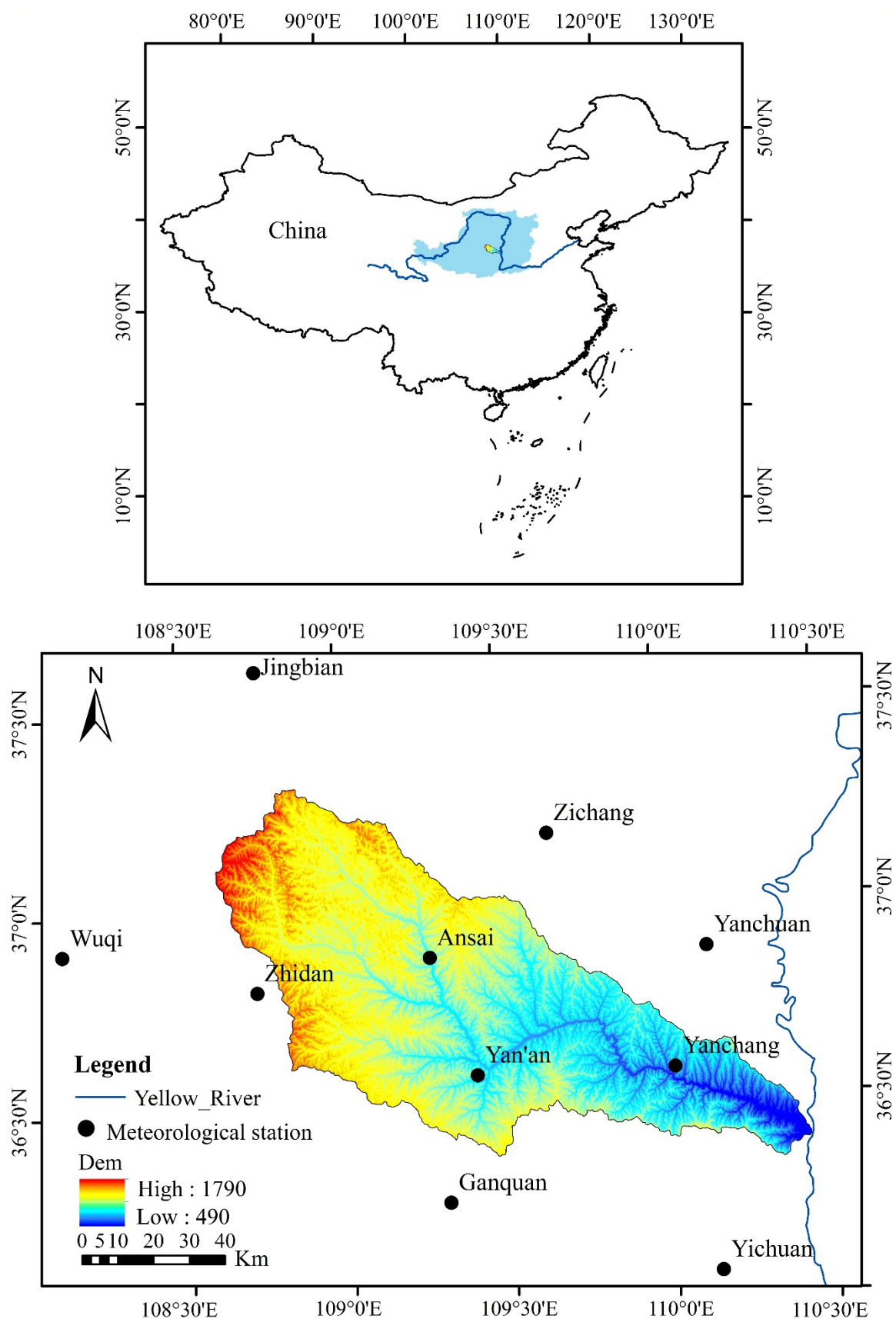


Figure 1 Location of the Yanhe River Basin and the meteorological stations used in this study (black dots).

599

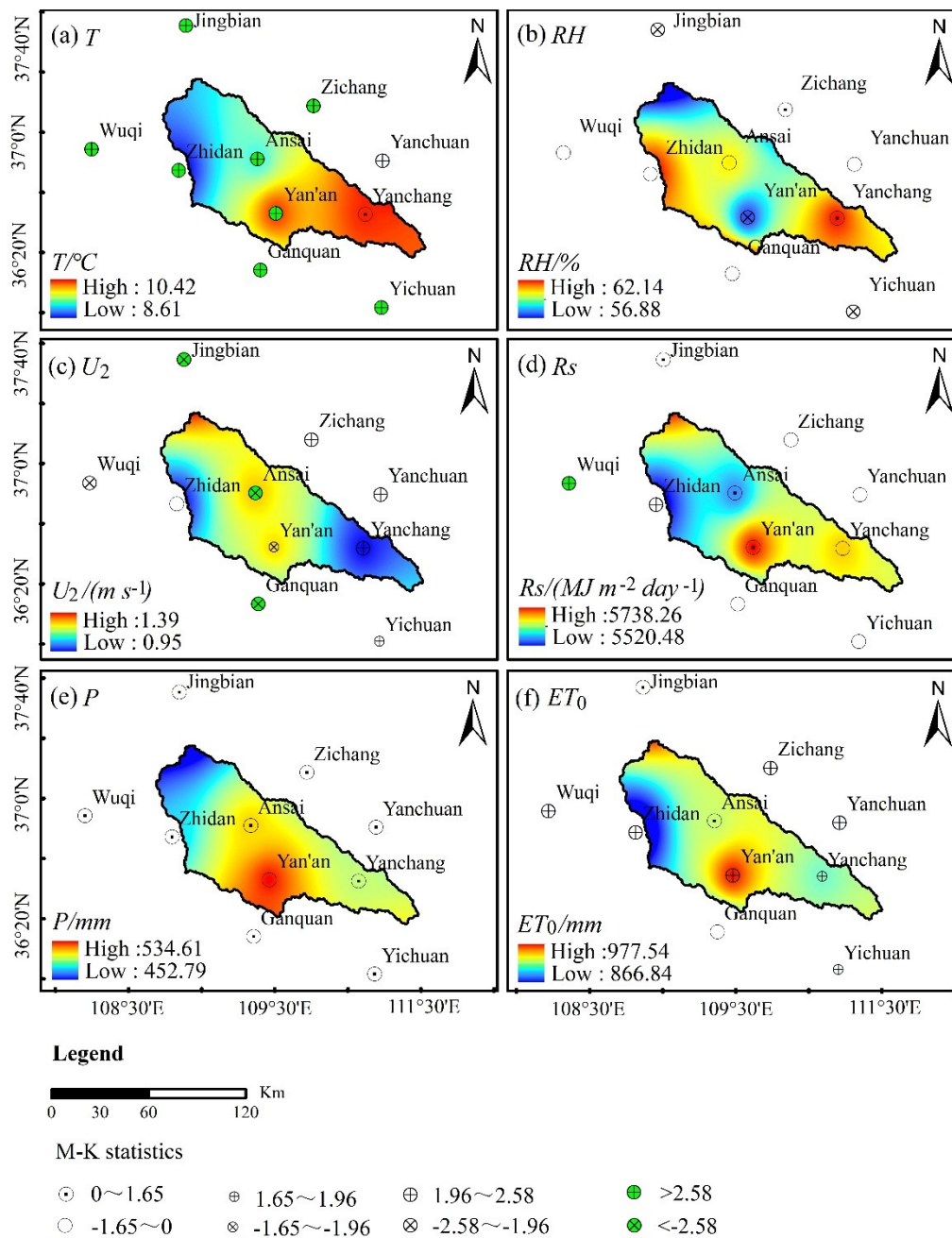


Figure 2 Spatial distribution of contribution rate of each meteorological factor.

602

603

604

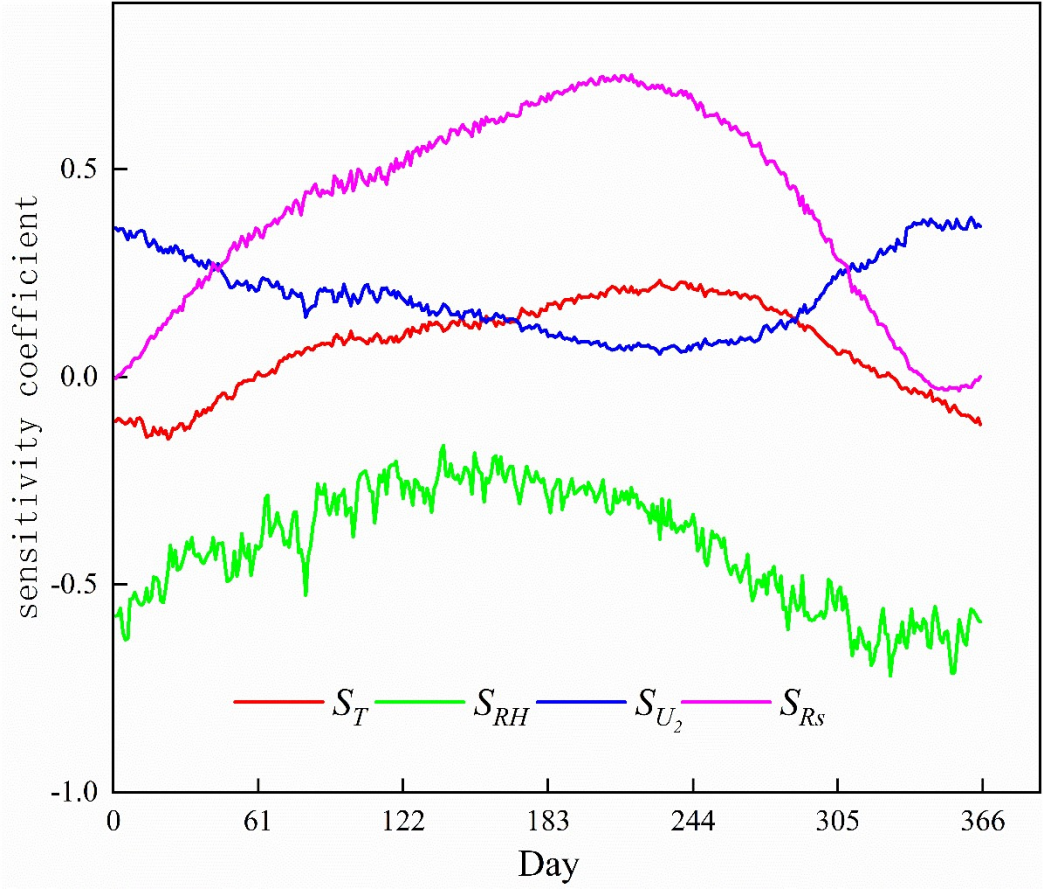
605

606

607

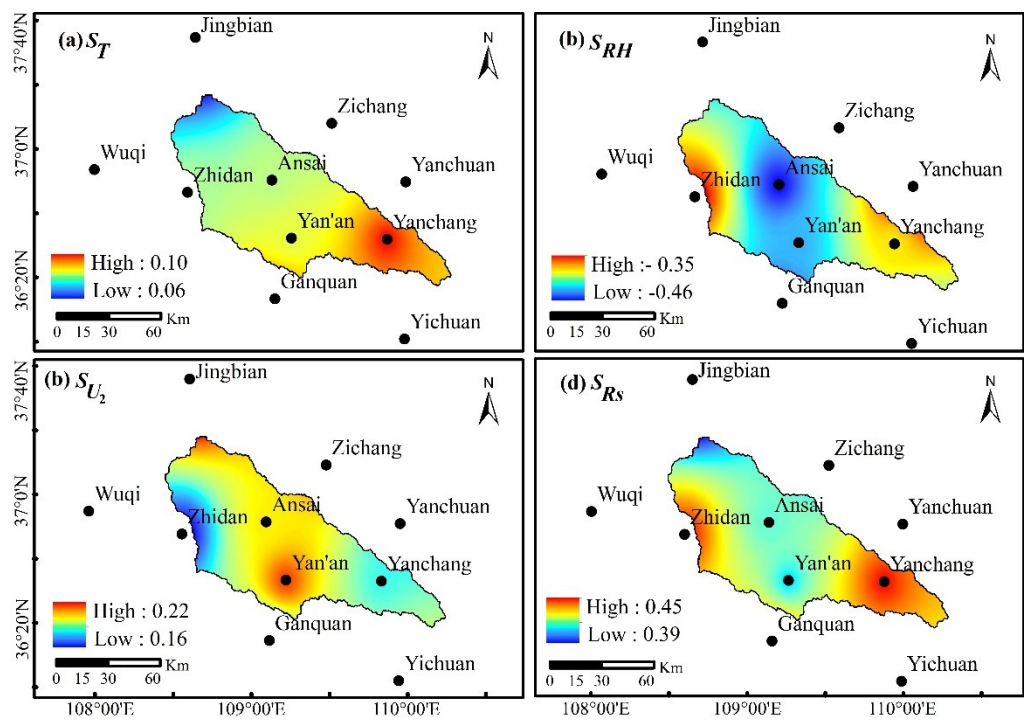
47

608
609



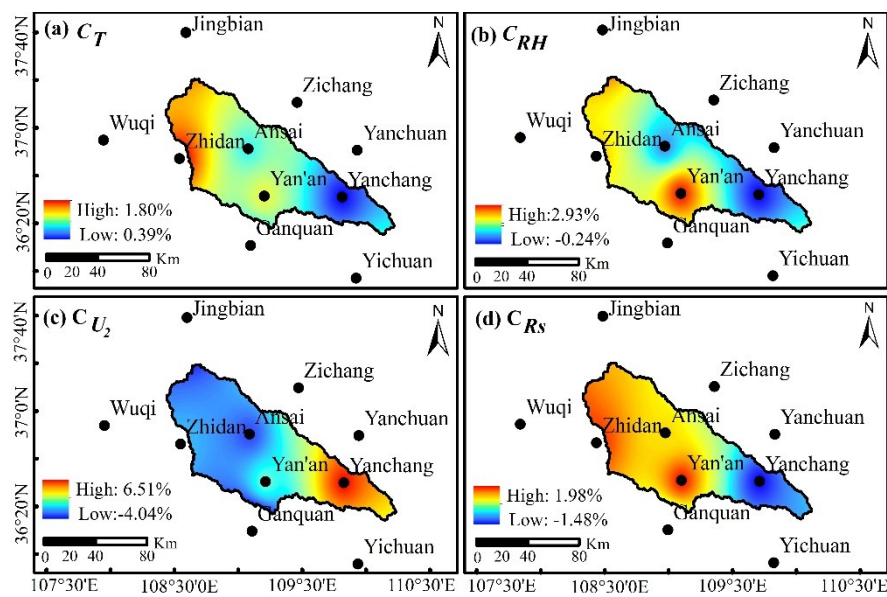
610
611
612
613
614
615
616
617
618
619
620
621
622
623
624

Figure 3 Characteristics of average daily sensitivity coefficient of ET_0 to meteorological



factors.
Figure 4 Spatial distribution of sensitivity coefficients of ET_0 to meteorological factors.

645



646

647

648

Figure 5 Spatial distribution of contribution rate of each meteorological factor.